

This is the peer reviewed version of the following article:

Anna Nadal, Anna Coll, Anna Aviñó, Teresa Esteve, Ramon Eritja, Maria Pla. “Efficient Sequence-Specific Purification of *Listeria innocua* mRNA Species by Triplex Affinity Capture with Parallel Tail-Clamps”. *ChemBiochem*, 2006, 7 (7): 1039-1047

Which has been published in final form at <https://doi.org/10.1002/cbic.200500519>

This article may be used for non-commercial purposes in accordance with Wiley Terms and Conditions for Use of Self-Archived Versions. This article may not be enhanced, enriched or otherwise transformed into a derivative work, without express permission from Wiley or by statutory rights under applicable legislation. Copyright notices must not be removed, obscured or modified. The article must be linked to Wiley’s version of record on Wiley Online Library and any embedding, framing or otherwise making available the article or pages thereof by third parties from platforms, services and websites other than Wiley Online Library must be prohibited.

Efficient sequence-specific purification of *Listeria innocua* mRNA species by triplex affinity capture with parallel tail-clamps

Anna Nadal ^[a], Anna Coll ^[a], Anna Aviñó ^[b], Teresa Esteve ^[c], Ramon Eritja ^[b] and Maria Pla*^[a,c]

^[a] Institute of Food and Agricultural Technology (INTEA). University of Girona, Campus Montilivi (Edif. Politècnica 1), Girona E-17071, Spain (phone: +34(972)419852; fax: +34(972)418399)

A. Nadal: anadal@intea.udg.es

A. Coll: anna.coll@udg.es

M.Pla: maria.pla@udg.es

^[b] Dpt. de Biologia Estructural, Institut de Biologia Molecular de Barcelona (IBMB), Consejo Superior de Investigaciones Científicas (CSIC), Jordi Girona 18-26, E-08034 Barcelona, Spain (phone: +34(93)4006145; fax: +34(93) 2045904)

A. Aviñó: aaagma@cid.csic.es

R. Eritja: recgma@cid.csic.es

^[c] Dpt. de Genètica Molecular, Consorci CSIC-IRTA, Jordi Girona 18-26, E-08034 Barcelona, Spain (phone: +34(93)4006100; fax: +34(93) 2045904)

T.Esteve: tengmp@ibmb.csic.es

* Corresponding author: Maria Pla.

Running Title: mRNA triplex affinity capture by tail-clamps

Abstract

Parallel clamps can interact in a sequence specific manner with homopyrimidine DNA and RNA oligonucleotides to form triplexes. For longer nucleic acids, we previously demonstrated the inhibitory effect of DNA target secondary structures on triplex formation. We further designed a modification of these molecules -i.e. tail-clamps by addition of a tail sequence to the parallel clamp- and proved its efficient binding with structured single-stranded DNA targets. Here we explored the possible application of the tail-clamp strategy for triplex formation with RNA targets; which are typically found as strongly folded single-stranded molecules. Efficient and specific binding of a tail-clamp designed to form a parallel triplex with *Listeria innocua iap* mRNA sequences was verified by UV melting curves and triplex affinity capture techniques. Furthermore, we show for the first time the formation of stable complexes of mRNA with tail-clamps not only at acidic but at neutral and slightly basic pH conditions. These results signify one step further towards possible applications of triplexes with mRNA molecules: research, analytical and also therapeutic uses can be envisaged. As an example, our tail-clamp-based triplex affinity capture assay allowed specific capture and recovery of *iap* mRNA molecules from a *L. innocua* total RNA solution with 45% yield.

Keywords

Triplex affinity capture RNA, parallel tail-clamps, mRNA purification, *Listeria*, structured target, RNA.

Introduction

There is a large interest in the design of sequence-specific DNA- and RNA-binding molecules that may have diagnostic or therapeutic value. It has been shown that oligonucleotides bind oligopurine-oligopyrimidine sequences of double-stranded DNA by forming triple-helical structures (triplexes). Depending of the orientation of the third strand with respect to the central oligopurine Watson-Crick strand, triplexes are classified into two main categories: parallel and antiparallel. The formation of parallel triplexes requires protonation of cytosine so they are most stable in acidic conditions. In contrast, antiparallel triplexes do not required protonation so they are stable at a broader pH conditions.^[1-5]

Sequence specific triple-helix structures can also be formed by DNA clamps. Parallel-stranded DNA clamps consist of purine residues linked to a homopyrimidine chain of inverted polarity by 3'-3' or 5'-5' internucleotide junctions^[6-8] which interact with single-stranded homopyrimidine nucleic acid targets.^[6,7,9,10] In this type of triplex, the homopurine strand binds the homopyrimidine target through Watson-Crick bonds; and the clamp homopyrimidine strand binds through Hoogsteen bonding and is stabilized under acidic conditions.^[1,11] The stability of triple helices has been enhanced by replacing natural bases with some modified bases such as 8-aminopurine residues.^[6,12]

Using the cauliflower mosaic virus 35S promoter sequence, we previously demonstrated^[13] the correlation of a secondary structure concerning the target (*in silico* predicted and experimentally confirmed) and an

inhibitory effect on triplex formation. We overcome structural impediments by designing a new type of clamps: tail-clamps, and demonstrated that parallel-tail-clamps^[13] efficiently form triple helices with structured single-stranded DNA target sequences.

RNA molecules are typically found as single stranded nucleic acids mostly fold in stable secondary structures. Short RNA oligonucleotides have been reported to form stable triple structures with parallel-stranded conventional clamps^[7,14] and with parallel-tail-clamps modified with 8-aminoadenine residues.^[13] Widening the scope of application of the tail-clamp strategy to triplex formation with long and structured mRNA targets would be highly desirable for its use as a new tool for applications such as research or diagnostic assays.^[1-5]

In this report, we synthesized parallel tail-clamps designed to bind with *Listeria innocua*^[15,16] *iap* mRNA sequences containing a polypyrimidine track within a region of strong predicted secondary structure. Our aim was to obtain the best conditions for the triplex affinity capture^[17-22] of *Listeria innocua iap* mRNA sequences in order to develop new detection methods for pathogens based on the specific detection of their nucleic acids. In our study we explored the effect of the pH on the interaction of parallel tail-clamps with their target by UV thermal melting analysis and we optimized a triplex affinity capture assay capable to capture and recover *iap* mRNA molecules from a total RNA solution purified from *L. innocua* cells in a sequence specific manner. Surprisingly, best results were obtained with tail-clamps carrying 8-

aminoadenine moieties at neutral pH conditions. This result is significant for the possible use of these clamps for diagnostic and therapeutic purposes.

Results and discussion

The main aim of the present study was to explore the possibilities of clamp-based parallel triple helix formation with real mRNA targets for diagnostic and therapeutic applications. Messenger RNA molecules tend to adopt secondary structures that have an effect on intermolecular interactions. We previously demonstrated that the tail-clamp strategy allowed triplex formation with single stranded DNA molecules displaying stable secondary structures. Here we report triplex formation with mRNA extracted from exponentially growing *L. innocua* cells. Moreover, we report the use of triplex for specific capture and recovery of *L. innocua* mRNA molecules. The system was initially studied and optimized by using as target a structured RNA transcript, which should represent a better model of real mRNA molecules than the short DNA or RNA oligonucleotides typically used in thermodynamic studies.^[6,13] Our RNA target was the *L. innocua iap* mRNA which contains a homopyrimidine track within a region of strong predicted secondary structure. Ten out of 12 target pyrimidine nucleotides were predicted to be involved in a stable stem (Watson-Crick intramolecular interactions) which break target ΔG value was calculated at $-8.0 \text{ kcal mol}^{-1}$. This stem was predicted when a 600-nt *iap* (nucleotides 390 to 990) mRNA fragment was analyzed; and also with a 147-nt fragment encompassing nucleotides 567 to 713 (i.e. *iap*-567). Therefore, *iap*-567 was selected as target in our initial triplex studies.

Thermal stability and hyperchromicity demonstrate triplex formation with *iap*-T-clamps and target oligonucleotides.

We designed and synthesized a parallel clamp (iap-clamp) and a parallel tail-clamp targeting the *iap* polypyrimidine track (iap-T-clamp). The parallel-stranded iap-clamp (Table 1) was designed carrying the purine sequence complementary to the *L. monocytogenes iap* homopyrimidine target sequence; connected head-to-head and through their 3'-ends with the Hoogsteen C,T-sequence. A tetrathymidine loop was used for connecting both strands. At one of the ends a biotin molecule was added to allow its capture by streptavidin. The parallel tail-clamp 3AA-iap-T-clamp (Table 1) had a similar composition, with the homopurine and the homopyrimidine parts connected through their 5' ends with the hexaethyleneglycol linker [(eg)₆] but 3 adenines were replaced by three 8-aminoadenines. Unm-iap-T-clamp has the same sequence than 3AA-iap-T-clamp but it does not contain modified 8-aminoadenine residues. 3AA-iap-T-clamp and unm-iap-T-clamp had 12 additional bases at the 3' end of their Watson-Crick forming strand. Such additional bases corresponded to the tail sequence and were complementary to the *L. monocytogenes iap* mRNA after the homopyrimidine track so these tail-clamp oligonucleotides could form a duplex and a partial triplex. A biotin molecule was also added at one of the ends. Previous work demonstrated that the position and the nature (tetrathymidine or hexaethylenglycol) of the loop did not produce any significant change on the binding of the clamps to their target.^[6] The orientation and nature of the loops were selected in each case to facilitate the synthesis of the clamps.

A parallel tail-clamp complementary to 35S CaMV promoter sequence (35S-T-clamp,^[13]) was used as a negative control to assess the selectivity of the binding. Finally, the biotinylated oligonucleotide sequence WCiap-T

was prepared. This oligonucleotide was complementary to the *L. monocytogenes iap* mRNA but the Hoogsteen forming strand was omitted and therefore could not form triplex.

We used UV-thermal melting techniques to analyze the binding of *Listeria* clamps in combination with a model DNA oligonucleotide target i.e. 32pyr (Figure 1). 32pyr included the 12 homopyrimidine and the tail target sequences; and no stable secondary structure was both *in silico* predicted (break target $\Delta G = 0$) and experimentally confirmed (no transition was observed with 32pyr alone). The thermal stability of the complex formed between 3AA-iap-T-clamp and 32pyr oligonucleotides at pH 5.0 (i.e. optimal pH conditions for parallel triplex formation,^[6]) showed two consecutive transitions (Table 2 and Figure 2). At higher pHs (pH 6-8) only one single transition was observed but melting curves were broad showing a complex behavior that could not be adjusted on a simple two-states curve-fitting model. The unmodified iap-T-clamp gave one broad transition at all studied pH (pH 5-8, Table 2). We next studied the effect of the Hoogsteen bonds on the tail-clamp / target binding by using the duplex-forming oligonucleotide (WCiap-T, Table 1) in which the Hoogsteen forming strand was omitted (Figure 1). As expected, Watson-Crick interactions occurred and displayed a single transition with lower T_m values than the one corresponding to the second transition of 3AA-iap-T-clamp (Table 2 and Figure 2). At pH 5.0 the hyperchromicity associated to the duplex transition was 17% while the hyperchromicity observed with the 3AA-iap-T-clamp and unm-iap-T-clamp was 25-26%. This supported the role of the Hoogsteen bonding in the iap-T-clamp and unstructured model target sequences at pH 5; as it occurred with other

tail-clamps.^[13] At neutral pH duplex-forming oligonucleotide (Wciap-T) had a slightly higher T_m compared to T_m observed for the triplex-forming oligonucleotides (3AA-iap-T-clamp and unm-iap-T-clamp) and hyperchromicities were similar: 21% (Wciap), 23-24% (unm-iap-T-clamp) and 26-28% (3AA-iap-T-clamp). In order to evaluate the formation of triplex at neutral pH further experiments were undertaken (see below). The melting curves of the complex between iap-clamp and 32pyr had a similar shape to 3AA-iap-T-clamp melting curves but melting temperatures and hyperchromocities were lower due to the shorter length and the absence of 8-aminoadenine residues.

The addition of magnesium has been reported to stabilize triple helices.^[1,4] In our system, the addition of 1 mM Magnesium did not yield any significant change in the T_m except for the transitions of the 3AA-iap-T-clamp and iap-clamp oligonucleotides at pH 5. In these melting experiments the double transition disappeared and a single broad transition was observed which displayed an apparent melting temperature between the two values observed in the experiment performed without magnesium (Table 3).

In order to assess the presence of triplex in the mixtures of clamps with their targets, melting curves were also analyzed at 300nm (Figure 3). Absorbance changes at longer wavelengths (i.e. 295-305 nm) have been described to indicate the formation of a nucleic acid structure which requires protonation / deprotonation of cytosines.^[23] At these wavelengths, the absorbance of protonated cytosines (such as cytosines within a triplex) is higher than the one of unprotonated cytosines. In this way a decrease in the absorbance at 300 nm upon heating may

indicate the presence of triplex. We observed that only the mixture of 3AA-iap-T-clamp and its target (32pyr) gave the expected decrease in the absorbance at 300 nm while the duplex-forming oligonucleotide (WCiap + 32 pyr) gave a small increase of the absorbance (Figure 3). Although the changes at 300 nm were small, we could estimate that the melting temperature of the triplex was close to the melting temperature observed at 260 nm. The hypochromicity of the transition at 300 nm was the highest at pH 5.0 and slowly decreased until pH 8.0 where the transition was difficult to appreciate. Also the value of the T_m estimated at 300 nm was slowly decreasing as expected for a parallel triplex because its stability depends on protonation of cytosine. The very slow decrease in the stability of this particular triplex is due to its high A-T content (66%) and the presence of the 8-aminoadenine residues.^[6,12,14] It is also important to notice that the T_m at pH 5.0 and 300 nm is higher than the T_m obtained at 260 nm and this is reversed at neutral pH as expected for the need of cytosine protonation for triplex stability. This behavior has not been observed before and it may be due to the presence of 8-aminoadenine residues although the unmodified clamp also shows a slightly higher T_m at pH 5.0 when monitored at 300 nm (Table 3).

The triplex transition at 300 nm for the unmodified unm-iap-T-clamp was observed at pH 5.0 and pH 6.0 but not at pH 7.0. This is in agreement with the absence of the triplex-stabilizing 8-aminoadenine residues.

Finally, the triplex transition at 300 nm is only observed at pH 5.0 for the mixture of iap-clamp and its target (32 pyr) as expected for shorter length and the absence of 8-aminoadenine residues.

Efficient and specific interaction of iap-T-clamp with a long and structured RNA transcript.

We next assessed the capacity of 3AA-iap-T-clamp to interact with long and structured RNA targets by using iap-567 RNA transcript (147 nt) and gel-shift analysis. Binding was established by the appearance of a radioactive band with less mobility than the one corresponding to the target alone (Figure 4). The percentages of shifted bands were calculated at each fold excess of tail-clamp and showed increasing amounts of complexes (i.e. 0 % at 0-, 68 % at 10- and 100 % at 50-fold). The specificity of binding was demonstrated by the non interaction of 3AA-iap-T-clamp and a 147-nt RNA molecule lacking the homopyrimidine target (Figure 4) i.e. iap-567(-), corresponding to the negative strand of iap-567. Furthermore, the same percentages of shifted bands were obtained in the presence of 1000-fold excess of other non-target RNA.

The efficiency of 3AA-iap-T-clamp and iap-567 binding was quantified by means of the kinetic association constant k_{obs} value; which corresponded to $3800 \text{ M}^{-1} \text{ s}^{-1}$. Remarkably, our previous studies with an equivalent parallel-tail-clamp and a short RNA oligonucleotide exhibited only slightly higher k_{obs} values than the ones obtained with 3AA-iap-T-clamp and the long and predictably tightly folded iap-567.^[13] Parallel experiments were conducted with iap-clamp (Table 1), a parallel-clamp corresponding to iap-T-clamp without the tail sequence. A non-tailed clamp had previously been shown to be unable to interact with strongly structured targets.^[13] Although iap-clamp efficiently formed triplex with the unstructured 32pyr oligonucleotide (see Figure 1 and Table 2);

it failed to interact with iap-567 at detectable levels ($k_{obs} = 0$) even at 50-fold excess clamp (Figure 4). These negative results are in agreement with the presence of a secondary structure in the target that interfered with non-tailed clamp based triplex formation. Our tail-clamp system efficiently overcame RNA structural impediments and bound long RNA molecules; and therefore its use for triplex formation with real mRNA molecules should be possible.

A triplex affinity capture assay allows specific recovery of *L. innocua* iap mRNA.

The specific interactions among two different molecules allow the development of research, diagnostic and therapeutic techniques. As an example, DNA molecules have been sequence-specific purified by "triplex affinity capture".^[17-22] We developed a triplex affinity capture assay based on 3AA-iap-T-clamp for the specific capture and recovery of iap mRNA molecules purified from *L. innocua* cells (see scheme in Figure 5). The obtained results could shed light on further possibilities of tail-clamps as an additional molecular tool for analytical purposes. The capture and recovery process was monitored by an RT-QPCR capable to quantitatively detect *L. innocua* iap sequences adjacent to the homopyrimidine triplex target.

The assay was initially developed by using iap-567 target, which contains both, triplex and RT-QPCR target sequences. At standard parallel triplex forming conditions we successfully captured and recovered closed to 18% iap-567 by means of affinity capture using 3AA-

iap-T-clamp (Table 4). No significant amounts of RNA target was found in the magnetic beads after elution (i.e. less than 0.01%). Thus, the method allowed the capture of structured RNA targets and its subsequent recovery. The specificity of the system was tested by performing a series of control experiments. First, the 3AA-iap-T-clamp was either omitted or substituted by an equivalent parallel-tail-clamp targeting at a completely different sequence (i.e. 35S-T-clamp^[13]). Recovery values obtained were at least two logarithmic units below the 3AA-iap-T-clamp values (Table 4), and were considered as background values. The specificity of the 3AA-iap-T-clamp based capture and recovery system was further verified by control experiments with non-target RNA molecules. We assayed iap-567(-), the negative strand of the target sequence; and also iap-520, an *in vitro* transcribed 150-nt RNA molecule corresponding to nt 520 to 670 of the same *iap* mRNA. iap-520 contains the RT-QPCR target sequence but not the triplex target homopyrimidine track. The capture of non-target RNA molecules by 3AA-iap-T-clamp produced recovery values closed to the background (Table 4). Finally, the same percentages of recovery were obtained in the presence of increasing amounts of unspecific nucleic acids (e.g. around 20% of recovery with 3AA-iap-T-clamp with up to 10⁶-fold molar excess RNA or DNA).

For a potential inclusion of tail-clamps in the analytical toolbox it would be desirable to increment the recovery yield of our triplex affinity capture assay. Tail-clamps are expected to interact with their RNA substrates through both, parallel-Hoogsteen and Watson-Crick bonds (Figure 1). Hoogsteen bonds in parallel triplexes are described to be

most stable at acidic pH^[6] whereas Watson-Crick bonds at neutral pH. Although less efficiently, duplex structures were also formed with our *iap* target sequence at pH 5.0 (see Table 2 and Figure 2) and triplex formation at less acidic pH should be possible. We determined the pH conditions at which the combination of parallel-Hoogsteen and Watson-Crick bonds resulted in the strongest affinity of 3AA-*iap*-T-clamp and the *iap* mRNA sequence; and therefore the highest yield of our capture and recovery assay could be achieved. We performed a comparative study on the recovery of *iap*-567 achieved with 3AA-*iap*-T-clamp at different pH (Table 4). Recovery values attained at neutral or slightly basic conditions were around 30% i.e. significantly higher than the ones at pH 5.0 and 6.0. Therefore, we used the optimal conditions at pH 7.0 to specifically capture and recover *iap* mRNA from total RNA extracted from *L. innocua* exponentially growing cells. Remarkably, our triplex affinity capture assay produced yields as high as 45% of the *iap* mRNA (45 ± 2 %). As it could be expected, non-target tail-clamps produced no recovery, further confirming the lack of unspecific binding to magnetic beads. We next further demonstrated the specificity of our capture and recovery system, and therefore we conclusively proved its suitability for sequence specific enrichment / purification of mRNA species: we monitored the levels of both, *iap* mRNA and a second *L. innocua* mRNA molecule, *lin02483* mRNA,^[24] along capture and recovery of *iap* mRNA from a total RNA solution prepared from *L. innocua* cells. The non-target *lin02483* mRNA produced recovery levels corresponding to background levels (i.e. below 0.1 %) while the target *iap* mRNA displayed recovery

values around 45 %. Thus, our affinity capture assay could be suitable for efficient sequence specific purification of mRNA species.

Significance of the formation of stable triplexes with mRNA at neutral pH.

The stability of parallel triplex structures has been described to be maximal at acidic pH and to strongly decrease at neutral or basic conditions. The pH effect on the stability of triplexes formed with tail-clamps has not been described to date. Due to the high content of T residues of the target it was expected that stability of the triplex would not be so much pH-dependent. Therefore, triplex formation in our affinity capture assay could not be excluded. For these reasons, we paid special attention to determine whether triplex structures were indeed formed in the conditions of our affinity capture assay.

The presence of two clear transitions at pH 5 (Figure 2) and the higher hyperchromicity observed during the denaturation of the complexes at 260 nm (Table 2) were indicative of the presence of triplex. But the most clear evidence of triplex formation at neutral pH was obtained by monitoring the melting process at 300 nm where a curve with negative slope indicated the presence of the triplex even at pH 7 (Figure 3, Table 3).

Affinity capture assays produced higher recovery values (around 2-fold) with 3AA-iap-T-clamp than WCIap-T along the whole pH range tested (Table 3). This suggested that triplex structures stabilized bimolecular interactions at acidic and also at neutral conditions. Interestingly, this phenomenon was added to the expected higher stability of Watson-

Crick bonding at neutral conditions; which resulted in the most stable parallel triplex structures by tail-clamps at physiological pH.

The results obtained by WClap-T and 3AA-iap-T-clamp confirmed that although Watson-Crick interactions do occur; Hoogsteen bonding has indeed a predominant role in the stability of tail-clamp / long RNA complexes even at neutral pH. This places our triplex affinity capture assay as a new tool for diagnostic applications: triplex effectively contributes to the overall stability of capture molecules - target mRNA interactions and results in higher yields as compared to duplex-based strategies. Finally, stable triplex formation at physiological conditions enables tail-clamps for use in a number of potential therapeutical applications. As an example, further experiments are currently carried out in order to assess their potential use for antisense inhibition of gene expression.

Experimental Section

Selection of a target *L. innocua* mRNA sequence for triplex based capture and recovery. RNA secondary structure prediction.

L. innocua are facultative anaerobic gram-positive bacteria widely distributed in the environment and frequently found in food products, where they can grow over a large pH and temperature ranges.^[15,16] The *L. innocua* virulence gene *iap* (LIN00591) encodes the invasion associated surface protein P60 (<http://genolist.pasteur.fr/ListiList/>) and its derived mRNA encompasses an adequate homopyrimidine track for triplex formation that we selected. It is 12 nucleotides long and located at positions 688 to 699 (according to Accession Number M80349) i.e. within a region of predicted strong secondary structure involving the target. The *iap*-567 RNA transcript (see below) was selected as target in our triplex study since (i) it contains the homopyrimidine track; (ii) such track is predicted to be embedded in the same stem as in the full-length *iap* mRNA; and (iii) it can be detected and quantified by the *iap* reverse transcription-real-time PCR (RT-QPCR) we developed (see below).

Single-stranded RNA structures were predicted using the *RNAstructure* program, version 4.11.^[25] The *oligowalk* tool of the same software^[26] was used to calculate the stability of bimolecular interactions as break target ΔG values.

Synthesis of unmodified oligonucleotides.

Oligonucleotides used in this study are listed in Table 1. Unmodified oligonucleotides were synthesized on an Applied Biosystems DNA

synthesizer model 392. Sequences were prepared using standard (Bz- or ibu-protected) 3'-phosphoramidites and polystyrene solid supports (LV200) following the protocols of the manufacturer. Coupling efficiencies were higher than 98%. After the assembly of the sequences, oligonucleotide-supports were treated with 32% aqueous ammonia at 55 °C for 16 h. Ammonia solutions were concentrated to dryness and the products were desalted on NAP-10 (Sephadex G-25) columns eluted with water. The length and homogeneity of the products was checked by denaturing polyacrylamide gel electrophoresis.

Synthesis of clamps

The parallel-stranded iap-clamp (Table 1) was designed carrying the purine sequence complementary to the *L. monocytogenes* iap homopyrimidine target sequence; connected head-to-head and through their 3'-ends with the Hoogsteen C,T-sequence. A tetrathymidine loop was used for connecting both strands. At one of the ends a biotin molecule was added to allow its capture by streptavidin.

The parallel tail-clamps 3AA-iap-T-clamp and unm-iap-T-clamp (Table 1) have a similar composition, with the homopurine and the homopyrimidine parts connected through their 5' ends with the hexaethyleneglycol linker [(eg)₆]. The 3AA-iap-T-clamp contained three 8-aminoadenines replacing three adenines. Both 3AA-iap-T-clamp and unm-iap-T-clamp have 12 additional bases at the 3' end of its Watson and Crick forming strand. Such additional bases correspond to the tail sequence and are complementary to the *L. monocytogenes* iap mRNA after the homopyrimidine track so these tail-clamp oligonucleotides will form a duplex and a

partial triplex. A biotin molecule was also added at one of the ends. A parallel tail-clamp complementary to 35S CaMV promoter sequence (35S-T-clamp,^[6]) was used as a negative control.

Oligonucleotides were prepared on an automatic Applied Biosystems 392 DNA synthesizer as described elsewhere.^[6] 5'-5' Clamps (3AA-iap-T-clamp and Unm-iap-T-clamp) were prepared in four steps. First, the purine part was assembled using standard phosphoramidites for the natural bases and the 8-aminoadenine phosphoramidites. The phosphoramidite of 8-aminoadenine was prepared as described elsewhere.^[6] Second, an hexaethyleneglycol linker was added using a commercially available phosphoramidite (Glen Research). Third, the pyrimidine part was prepared using reversed C and T phosphoramidites. And finally, biotin was added at the end of the sequence using a commercially available 5'-biotin phosphoramidite (Glen Research). The same protocol was used for the synthesis of the 35S-T-clamp. For the preparation of 3'-3' clamp (iap-clamp), a similar approach was used. In this case, the pyrimidine part was assembled first on 3'-biotin controlled pore glass support (Glen Research), followed by the tetrathymidine loop. Both parts were assembled using reversed phosphoramidites. The purine part was the last to be assembled using standard phosphoramidites. After the assembly of the sequences, oligonucleotide-supports were treated with aqueous ammonia (32%) at 55°C for 16 h. Ammonia solutions were concentrated to dryness and the products were purified by reversed-phase HPLC. Oligonucleotides were synthesized on a 200 nmol scale using polystyrene supports and with the last DMT group at the 5' end (DMT on protocol) to facilitate reversed-phase purification. All purified products presented

a major peak, which was collected. Yields (OD units at 260 nm after HPLC purification) were around 10 OD. HPLC conditions were as follows. Solvent A: acetonitrile (5%) in triethylammonium acetate pH 6.5 (100 mM) and solvent B: acetonitrile (70%) in triethylammonium acetate pH 6.5 (100 mM). Columns: PRP-1 (Hamilton), 250 x 10 mm. Flow rate: 3 ml/min. Linear gradients: 30 min 10-80% B (DMT on) or 30 min 0-50% B (DMT off). Oligonucleotide sequence WCiap-T contains the complementary sequence to the *L. monocytogenes iap* mRNA but the Hoogsteen forming strand was omitted. Biotin was added at the 5'-end using a commercially available 5'-biotin phosphoramidite (Glen Research). This oligonucleotide can only form a duplex with target sequence. The oligonucleotide was synthesized and purified as described above.

Binding of clamps to target sequences by melting experiments

Melting experiments were performed as follows. Solutions of equimolar amounts of clamps and the target strand were mixed in sodium phosphate/citric acid buffer (0.1 M) at the pH 5.0 and pH 6.0 or in sodium phosphate buffer (0.1 M) at the pH 7.0 and pH 8.0. In some cases, magnesium chloride (1 mM) was added. The DNA concentration was determined by UV absorbance measurements (260 nm) at 90°C, using for the DNA coil state the following extinction coefficients: 7500, 8500, 12500, 15000 and, 15000 M⁻¹ cm⁻¹ for C, T, G, A and, 8-amino-A, respectively. The solutions were heated to 90 °C, allowed to cool slowly to room temperature, and stored at 4°C until UV was measured. UV absorption spectra and melting experiments (absorbance vs temperature) were recorded in 1 cm path-length cells using a spectrophotometer, with a

temperature controller and a programmed temperature increase rate of 0.5 °C/min. Melts were run by duplicate on triplex concentration of 3 µM at 260 nm.

Melting curves were first analyzed by computer-fitting the denaturation data, using Meltwin 3.5 software but melting curves of the clamps did not adjust to a simple two-species model. For this reason, the melting temperatures were obtained as the maxima of the first derivative of the melting curves. On the basis of multiple experiments, the uncertainty in T_m values was estimated at +/- 1 °C except for transitions followed at 300 nm in which the uncertainty in T_m values was estimated at +/- 2 °C.

Preparation of target RNA transcripts

iap-567, *iap-567(-)* and *iap520* were obtained by *in vitro* transcription from PCR products performed with *L. innocua* genomic DNA and primers T7*iap-567f* and *iap-713r*; primers *iap-567f* and T7*iap-713r*; and primers T7*iap-520f* and *iap-670r*, respectively (Table 1). To obtain RNA target, DNA template (1 µg) was transcribed *in vitro* for 1 h at 37°C (with [α -³²P]-GTP for radio-labelled transcript) followed by a 5 min treatment with RNase-free DNase I at 37°C. Cellulose CF11 chromatography was used to eliminate DNA fragments and non-incorporated nucleotides. The transcript was then purified by gel electrophoresis under denaturing conditions on a polyacrylamide (4%) gel containing urea (7 M). The band was visualized by autoradiography, excised from the gel and eluted in TE buffer (100 mM Tris-HCl and 10 mM EDTA) pH 7.5. The concentration of cold transcripts was determined by spectrophotometry using the NanoDrop device (NanoDrop Technologies, Delaware, USA). Radioactive transcript

was quantified by calculating the amount of incorporated [α -³²P]-GTP based on scintillation counting.

Total RNA extraction from *L. innocua* cells

Bacterial nucleic acids were extracted from overnight cultures of *L. innocua* strain CECT910 grown in brain heart infusion broth medium (Oxoid, Hampshire, UK) by use of the High Pure RNA Isolation kit (Roche Applied Science, Penzberg, Germany) according to the manufacturer's recommendations. Nucleic acid concentration was determined by spectrophotometry using the NanoDrop ND-1000 device (NanoDrop Technologies, Delaware, USA).

Standard conditions for triplex formation

Targets were heated at 93°C for 3 min in buffer A (0.1 M sodium phosphate/citric acid) pH 5.0 (pH 6.0, 7.0 and 8.0 were also used for pH comparative studies); and cooled on ice for 1 min. The *iap* clamps were added, and the samples were incubated at room temperature in a final volume reaction of 10 μ l for 1 h.

Gel electrophoretic mobility shift analysis of the triplex formation

Gel-shift experiments were performed as previously described^[13] using radio-labeled *iap*-567 or *iap*-567(-) target (25 fmol) and increasing amounts (i.e. 0-, 10- and 50-fold) of clamp. Triplexes were allowed to form in buffer A pH 5.0; and were resolved in non-denaturing polyacrylamide gels (4%) in the same buffer run at 4°C. The formation of triplex was monitored by the appearance of a radioactive band with less

mobility than the one corresponding to the target alone. Gels were scanned on a phosphorimager (Molecular Dynamics) and shifted and non-shifted bands were quantified using ImageQuant software (Molecular Dynamics). The observed kinetic association constants k_{obs} were estimated by calculating the ratio of the shifted bands vs. total target (shifted plus non-shifted bands) at a 10-fold molar excess clamp in a minimum of 3 independent experiments. Standard deviations were in all cases around 10%.

Triplex affinity capture

Streptavidin-coated magnetic beads (4 μ l Dynabeads M270 Streptavidin, Dynal Biotech, Oslo, Norway) were thoroughly washed in buffer B (1 M NaCl, 0.1 M sodium phosphate/citric acid) pH 5.0 (pH 6.0, 7.0 and 8.0 were also used for pH comparative studies). They were subsequently incubated with 50-fold excess biotinylated clamps in a final volume of 10 μ l of buffer A at the corresponding pH for 30 min at room temperature. The beads were separated by use of a magnetic particle concentrator (Dynal Biotech, Oslo, Norway) and were washed 3 times with buffer A. They were saturated with tRNA (3 μ l of 10 μ M) in buffer A for 5 min; and incubated with the appropriate molecular amounts of target in a final volume of 13 μ l at room temperature for 1 h. For transcript RNA targets, 150 fmol (corresponding to approximately 10^{11} molecules) were used; whereas for *L. innocua* total RNA solutions we used 10^9 *iap* mRNA molecules (i.e. approximately $1/25^{\text{th}}$ mRNA extracted from 1 ml culture). After thoroughly washing with the same buffer, elution of the target was

achieved by incubation in Tris buffer (0.1M) pH 8.0 at 90°C for 10 minutes.

The process was monitored by reverse-transcription (RT-) and real-time (Q) PCR quantification. The RNA transcript was quantified at 3 different stages: a) at the time zero of the triplex formation reaction to normalize the recovery values; b) in the recovery buffer; and c) in the magnetic beads after elution. The efficiency of capture and recovery of the method were expressed as percentages of recovered target (b) vs. initial sample (a). The process was performed in 5 independent experiments.

***iap* specific QPCR and RT-QPCR**

Sequence-specific QPCR and RT-QPCR assays were designed and evaluated essentially as described^[24] with TaqMan PCR core reagents (Applied Biosystems-Roche Molecular Systems Inc., Branchburg, N.J.). Reactions performed in a 10- μ l volume contained PCR TaqMan buffer A (1 \times , including 5-carboxy-Xrhodamine [ROX] as a passive reference dye); MgCl₂ (5 mM); dATP, dCTP, and dGTP (200 μ M each); dUTP (400 μ M); *iapQf* primer (900 nM) and *iapQr* primer (300 nM); *iapQp* probe 100 nM) (Table 1); AmpliTaq Gold DNA polymerase (1 U); AmpErase uracil *N*-glycosylase (0.2 U); and the target DNA solution (1 μ l). Reactions were run on an ABI Prism 7700 apparatus (Applied Biosystems Division, Perkin-Elmer) with the following program: 2 min at 50°C, 10 min at 95°C, and 40 cycles of 15 s at 95°C and 1 min at 60°C. The reverse transcription was optimized to be included in the same QPCR tube by adding 2.5 U of Moloney murine leukemia virus reverse transcriptase (Applied Biosystems-Roche Molecular

Systems Inc., Branchburg, N.J.) and substituting the initial 50°C incubation by 30 min at 42°C. QPCR and RT-QPCR assays were evaluated by using sequence detection system software, version 1.7 (Applied Biosystems Division, Perkin-Elmer). Quantification was performed by interpolation in a standard regression curve of threshold cycle (C_T) values generated from DNA or RNA samples at known concentrations. Negative values or a lack of amplification was set at a C_T value of 40. Unless otherwise stated, all reactions were performed in triplicate.

Acknowledgements

This work was supported by the Spanish Ministerio de Ciencia y Tecnología (grant INIA CAL01-058-C2-2 and BFU2004-02048), the "Fundació la Caixa" (BM04-52-0) and the "La Marató de TV3" Foundation. We thank Prof. Pere Puigdomènech and Dr. Jordi Gómez for valuable suggestions.

References

- [1] N. T. Thuong, C. Hélène, *Angew.Chem.Int.Ed.Engl.* **1993**, *32*, 666-690.
- [2] P. P. Chan, P. M. Glazer, *J.Mol Med.* **1997**, *75*, 267-282.
- [3] K. M. Vazquez, J. H. Wilson, *Trends Biochem.Sci.* **1998**, *23*, 4-9.
- [4] V. N. Soyter, V. N. Potaman, *Triple helical nucleic acids*, Springer-Verlag, New York, **1996**.
- [5] C. Malvy, A. Harel-Bellan, L. L. Pritchard, *Triplex helix forming oligonucleotides*, Kluwer Academic Publishers, Dordrecht, **1999**.
- [6] A. Aviñó, M. Frieden, J. C. Morales, B. G. de la Torre, R. Güimil-García, F. Azorín, J. L. Gelpí, M. Orozco, C. González, R. Eritja, *Nucleic Acids Res.* **2002**, *30*, 2609-2619.
- [7] E. R. Kandimalla, S. Agrawal, *Biochemistry* **1996**, *35*, 15332-15339.
- [8] J. H. van de Sande, N. B. Ramsing, M. W. Germann, W. Elhorst, B. W. Kalisch, E. von Kitzing, R. T. Pon, R. C. Clegg, T. M. Jovin, *Science* **1988**, *241*, 551-557.
- [9] A. Aviñó, J. C. Morales, M. Frieden, B. G. de la Torre, R. G. Garcia, E. Cubero, F. J. Luque, M. Orozco, F. Azorin, R. Eritja, *Bioorg.Med.Chem.Lett.* **2001**, *11*, 1761-1763.
- [10] E. Cubero, A. Avino, B. G. de la Torre, M. Frieden, R. Eritja, F. J. Luque, C. Gonzalez, M. Orozco, *J.Am.Chem.Soc.* **2002**, *124*, 3133-3142.
- [11] H. E. Moser, P. B. Dervan, *Science* **1987**, *238*, 645-650.
- [12] A. Aviñó, E. Cubero, C. Gonzalez, R. Eritja, M. Orozco, *J.Am.Chem.Soc.* **2003**, *125*, 16127-16138.
- [13] A. Nadal, R. Eritja, T. Esteve, M. Pla, *ChemBiochem* **2005**, *6*, 1034-1042.
- [14] A. Aviñó, M. G. Grimau, M. Frieden, R. Eritja, *Helvetica Chimica Acta* **2004**, *87*, 303-316.
- [15] P. Glaser, L. Frangeul, C. Buchrieser, C. Rusniok, A. Amend, F. Baquero, P. Berche, H. Bloecker, P. Brandt, T. Chakraborty, A. Charbit, F. Chetouani, E. Couve, A. de Daruvar, P. Dehoux, E. Domann, G. Dominguez-Bernal, E. Duchaud, L. Durant, O. Dussurget, K. D. Entian, H. Fsihi, F. Garcia-Del Portillo, P. Garrido, L. Gautier, W. Goebel, N. Gomez-Lopez, T. Hain, J.

- Hauf, D. Jackson, L. M. Jones, U. Kaerst, J. Kreft, M. Kuhn, F. Kunst, G. Kurapkat, E. Madueno, A. Maitournam, J. M. Vicente, E. Ng, H. Nedjari, G. Nordsiek, S. Novella, B. de Pablos, J. C. Perez-Diaz, R. Purcell, B. Rimmel, M. Rose, T. Schlueter, N. Simoes, A. Tierrez, J. A. Vazquez-Boland, H. Voss, J. Wehland, P. Cossart, *Science* **2001**, *294*, 849-852.
- [16] E. T. Ryser, E. H. Marth, *Listeria, listeriosis, and food safety*, Marcel Dekker, Inc., New York, N.Y., **1999**.
- [17] N. Bianchi, C. Rutigliano, M. Passadore, M. Tomassetti, L. Pippo, C. Mischiati, G. Feriotto, R. Gambari, *Biochem.J.* **1997**, *326*, 919-927.
- [18] T. Ito, C. L. Smith, C. R. Cantor, *Proc.Natl.Acad.Sci.U.S.A* **1992**, *89*, 495-498.
- [19] H. Ji, L. M. Smith, *Anal.Chem.* **1993**, *65*, 1323-1328.
- [20] A. F. Johnson, R. Wang, H. Ji, D. Chen, R. A. Guilfoyle, L. M. Smith, *Anal.Biochem.* **1996**, *234*, 83-95.
- [21] T. Kishida, M. Fukuda, K. Okazaki, W. Wang, Y. Tamaki, *Nippon Hoigaku Zasshi* **1996**, *50*, 255-257.
- [22] S. V. Sonti, M. C. Griffor, T. Sano, S. Narayanswami, A. Bose, C. R. Cantor, A. P. Kausch, *Nucleic Acids Res.* **1995**, *23*, 3995-3996.
- [23] J. L. Mergny, L. Lacroix, *Nucleic Acids Research* **1998**, *26*, 4797-4803.
- [24] D. Rodríguez-Lázaro, M. Hernández, M. Scotti, T. Esteve, J. A. Vázquez-Boland, M. Pla, *Appl.Environ.Microbiol* **2004**, *70*, 1366-1377.
- [25] D. H. Mathews, M. D. Disney, J. L. Childs, S. J. Schroeder, M. Zuker, D. H. Turner, *Proc.Natl.Acad.Sci.U.S.A* **2004**, *101*, 7287-7292.
- [26] D. H. Mathews, M. E. Burkard, S. M. Freier, J. R. Wyatt, D. H. Turner, *RNA.* **1999**, *5*, 1458-1469.

Figure legends

Figure 1. Schematic representation of the theoretical interactions between *iap* tail-clamps and their target sequences.

Figure 2. A) UV melting profiles (260 nm) for the triplex *iap*-T-clamp + 32 pyr and the duplex W*ciap* + 32 pyr at pH 5.0 (0.1M sodium phosphate-citric acid). **B)** First derivative of the corresponding melting curves. The normalized absorbance was obtained by dividing the observed absorbance by the absorbance at 20 °C.

Figure 3. UV melting profiles (300 nm) for the triplex 3AA-*iap*-T-clamp + 32 pyr and the duplex W*ciap* + 32 pyr at pH 7.0 (0.1M sodium phosphate-citric acid, 1 mM Mg²⁺). The melting curve of the triplex 3AA-*iap*-T-clamp + 32 pyr show a decrease on the absorbance at 300 nm at higher temperatures that are indicative of triplex transitions while the melting curve of the duplex W*ciap* + 32 pyr shows an increase of the absorbance at 300 nm.

Figure 4. *iap*-T-clamp specifically binds structured *iap* RNA fragments.

Autoradiograph of non-denaturing 4% polyacrylamide gel run at 4°C showing specific binding of 3AA-*iap*-T-clamp to *iap*-567. Twenty-five fmol ³²P-labelled RNA fragments were incubated with 50 molar equivalents of cold 3AA-*iap*-T-clamp (lanes 3 and 5) or *iap*-clamp (lane 2). Lanes 1-3, *iap*-567. Lanes 4 and 5, *iap*-567(-). Lanes 1 and 4, control reactions lacking tail-clamp.

Figure 5. Triplex-mediated capture and recovery of an mRNA target.

Scheme of the developed triplex affinity capture assay based on tail-clamps and structured RNA molecules. The secondary structure of RNA shown in the figure is a schematic representation of a RNA molecule.

TABLES

Table 1. Oligonucleotides used in this study.

name	use	sequence
3AA-iap-T-clamp	Triplex	biotin- ^{3'} TCTTCTTCTTCT ^{5'} - (eg) ₆ - ^{5'} AGAAGAAGAAGATAAAATTATTCCA ^{3'}
Unm-iap-T-clamp	Triplex	biotin- ^{3'} TCTTCTTCTTCT ^{5'} - (eg) ₆ - ^{5'} AGAAGAAGAAGATAAAATTATTCCA ^{3'}
iap-clamp	Triplex(short clamp)	biotin- ^{5'} TCTTCTTCTTCT-TTTT ^{3'} - ^{3'} AGAAGAAGAAGA ^{5'}
WCiap-T	Duplex (control)	biotin- ^{5'} AGAAGAAGAAGATAAAATTATTCCA ^{3'}
35S-T-clamp	Unrelated clamp	biotin- ^{3'} TCTTCTTTTTC ^{5'} - (eg) ₆ - ^{5'} GGAAAAAGAAGACGTTCCAACC ^{3'}
32pyr	DNA Target	^{5'} <u>TGGAATAATTTATCTTCTTCTTCT</u> ATTTATGT ^{3'}
T7 <i>iap</i> -567f <i>iap</i> -713r	Synthesis of <i>iap</i> -567	^{5'} taatacgactcactataggAGAAGCTCCAGTAGTAGA ^{3'} ^{5'} TGACCTACATAAATAGAA ^{3'}
<i>iap</i> -567f T7 <i>iap</i> -713r	Synthesis of <i>iap</i> -567(-) (control)	^{5'} AGAAGCTCCAGTAGTAGA ^{3'} ^{5'} taatacgactcactataggTGACCTACATAAATAGAA ^{3'}
T7 <i>iap</i> -520f <i>iap</i> -670r	Synthesis of <i>iap</i> -520 (control)	^{5'} taatacgactcactataggCCAACTACACAACAACTGCT ^{3'} ^{5'} TAATATCTTGAACAGAAACACCG ^{3'}
<i>iap</i> Qf <i>iap</i> Qr <i>iap</i> Qp*	QPCR and QRT-PCR	^{5'} AACGTTAAAAGCGGCGACAC ^{3'} ^{5'} AATATCTTGAACAGAAACACCGTACTTC ^{3'} ^{5'} 6-FAM-CGGATAATGCCCAA-MGBNFQ ^{3'}

A: 8-aminoadenine; (eg)₆:hexa(ethyleneglycol); : tail target sequence; :12 homopyrimidine target sequence; *oligonucleotide from commercial sources MGBNFQ: minor groove binding (MGB) probe with non-fluorescent quencher (NFQ); FAM: fluorescein label.

Table 2. Melting temperatures (T_m s) and hyperchromicity (H) of triplexes and duplexes in 0.1M sodium phosphate and citric acid at the appropriate pH. Each individual molecule was analyzed as control at pH 5.0: 3AA-iap-T-clamp: T_m 48.6°C; Unm-iap-T-clamp: T_m 46.3°C; iap-clamp, WCIap-T and target 32pyr: no transition was observed.

Clamp	T_m (°C)				H (%)			
	pH 5.0 ^[a]	pH 6.0	pH 7.0	pH 8.0	pH 5.0 ^[a]	pH 6.0	pH 7.0	pH 8.0
3AA-iap-T-clamp	48.5 and 57.0 ^[b]	53.2	55.4	58.7	25	28	28	26
Unm-iap-T-clamp	51.2	53.7	56.4	57.3	26	25	23	24
iap-clamp	30.8 and 47.1 ^[b]	36.6	34.7	40.1	15	11	13	14
WCIap-T	51.4	55.2	59.1	61.8	17	18	21	21

^[a] Uncertainties in T_m values are estimated at ± 1 °C.

^[b] Two transitions were observed.

Table 3. Melting temperatures (T_m s) of triplexes and duplexes in 0.1M sodium phosphate and citric acid containing 1 mM Mg^{2+} at the appropriate pH. Melting temperatures were obtained as the maxima of the first derivative of the melting curves using 3 μ M concentration.

Clamp	T_m (260 nm)				T_m (300 nm)			
	pH 5.0 ^[a]	pH 6.0	pH 7.0	pH 8.0	pH 5.0 ^[a]	pH 6.0	pH 7.0	pH 8.0
3AA-iap-T-clamp	51.8	52.3	54.6	58.0	55.0	54.0	51.0	– ^[b]
Unm-iap-T-clamp	50.7	53.9	56.5	57.0	52.0	48.0	– ^[b]	– ^[b]
iap-clamp	43.2	34.6	32.5	40.0	40.0	– ^[b]	– ^[b]	– ^[b]
WCiap-T	50.8	54.3	58.9	61.1	– ^[b]	– ^[b]	– ^[b]	– ^[b]

^[a] Uncertainties in T_m values are estimated at ± 1 °C, , except for transitions measured at 300 nm that are estimated ± 2 °C.

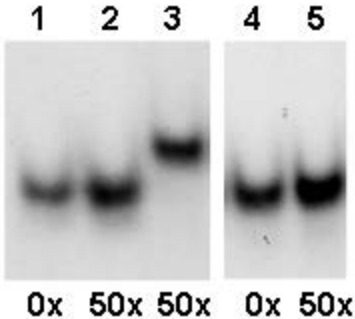
^[b] No transition was observed.

Table 4. Percentage of recovery of *iap*-567 target RNA by tail-clamp based triplex affinity capture. Results are means of at least 3 independent experiments. Standard deviations were consistently around 10%.

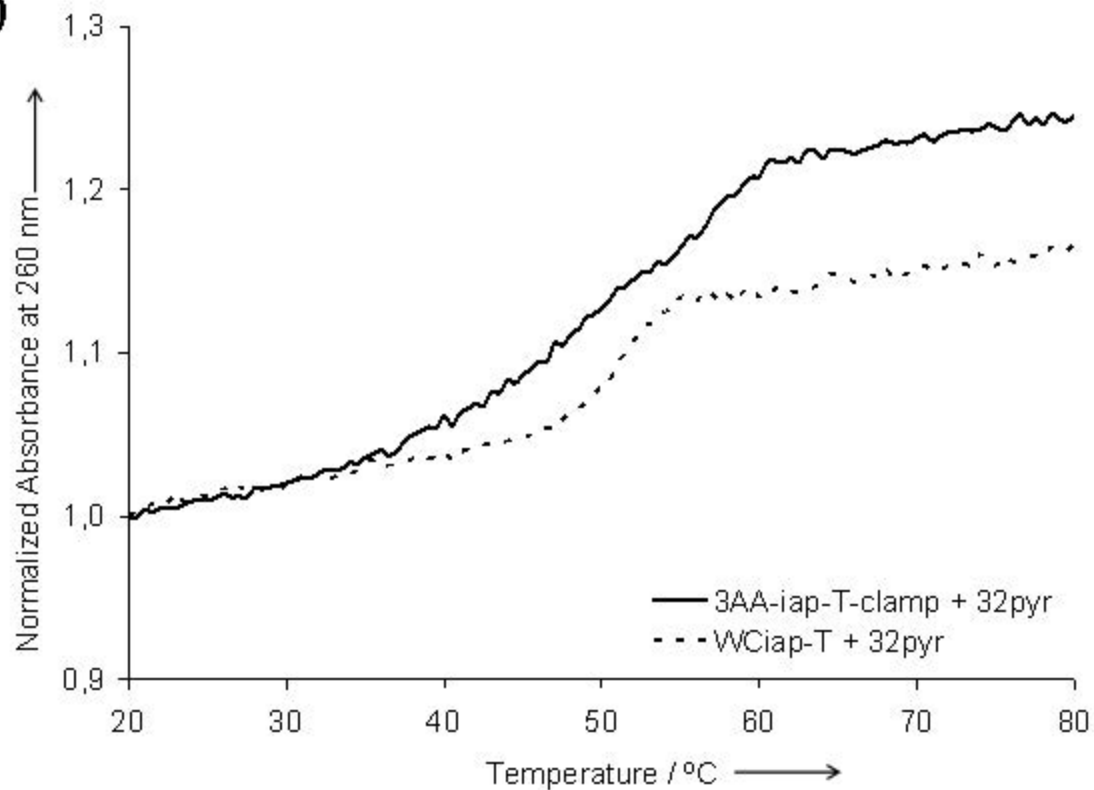
Tail-clamp	Target RNA	pH	Recovery ^[a]	Triplex/Duplex ^[b]
-	<i>iap</i> -567 alone	5.0	0.2	-
35S-T-clamp	<i>iap</i> -567	5.0	0.1	-
3AA- <i>iap</i> -T-clamp	<i>iap</i> -567 (-)	5.0	0.1	-
3AA- <i>iap</i> -T-clamp	<i>iap</i> -520	5.0	0.1	-
		5.0	18	2.0
	<i>iap</i> -567	6.0	19	1.9
3AA- <i>iap</i> -T-clamp		7.0	30	2.3
		8.0	29	2.4
	<i>iap</i> mRNA	7.0	45	2.0
		5.0	9	1.0
	<i>iap</i> -567	6.0	10	1.0
WC <i>iap</i> -T		7.0	13	1.0
		8.0	12	1.0
	<i>iap</i> mRNA	7.0	22	1.0

^[a] Recovery was calculated by RT-QPCR. This assay was linear along 5 logarithmic units (i.e. 10^5 to 10^9 initial target RNA molecules per reaction) with R^2 values above 0.99 and efficiency values of 0.93. For RNA quantification, residual target DNA template was systematically quantified by the corresponding QPCR assay (performance values, $R^2 = 0.99$ and $E = 0.95$) and always kept below 0.3 % of the transcribed RNA.

^[b] Recovery using 3AA-*iap*-T-clamp / recovery using WC*iap* in the same conditions.



**Clamp molar
equivalents**

A)

B)